Acta Biomaterialia 113 (2020) 350–359

Contents lists available at ScienceDirect

Acta Biomaterialia

journal homepage: www.elsevier.com/locate/actbio

Full length article

Hierarchical fibrous guiding cues at different scales influence linear neurite extension

Abdolrahman Omidinia-Anarkoli[a,b,c], John Wesley Ephraim[a], Rahul Rimal[a,b], Laura De Laporte[a,b,c,*]

[a] DWI-Leibniz Institute for Interactive Materials, Aachen 52074, Germany
[b] Institute of Technical and Macromolecular Chemistry, RWTH Aachen University, Aachen 52074, Germany
[c] Department of Advanced Materials for Biomedicine, Institute of Applied Medical Engineering, RWTH Aachen University, Aachen 52074, Germany

ARTICLE INFO

Article history:
Received 8 March 2020
Revised 4 July 2020
Accepted 7 July 2020
Available online 11 July 2020

Keywords:
SAS fibers
Fiber spinning
Topography
Nerve cell orientation
Nerve cell branching
Neurite extension

ABSTRACT

Surface topographies at micro- and nanoscales can influence different cellular behavior, such as their growth rate and directionality. While different techniques have been established to fabricate 2-dimensional flat substrates with nano- and microscale topographies, most of them are prone to high costs and long preparation times. The 2.5-dimensional fiber platform presented here provides knowledge on the effect of the combination of fiber alignment, inter-fiber distance (IFD), and fiber surface topography on contact guidance to direct neurite behavior from dorsal root ganglia (DRGs) or dissociated primary neurons. For the first time, the interplay of the micro-/nanoscale topography and IFD is studied to induce linear nerve growth, while controlling branching. The results demonstrate that grooved fibers promote a higher percentage of aligned neurite extension, compensating the adverse effect of increased IFD. Accordingly, maximum neurite extension from primary neurons is achieved on grooved fibers separated by an IFD of 30 μm, with a higher percentage of aligned neurons on grooved fibers at a large IFD compared to porous fibers with the smallest IFD of 10 µm. We further demonstrate that the neurite "decision-making" behavior on whether to cross a fiber or grow along it is not only dependent on the IFD but also on the fiber surface topography. In addition, axons growing in between the fibers seem to have a memory after leaving grooved fibers, resulting in higher linear growth and higher IFDs lead to more branching. Such information is of great importance for new material development for several tissue engineering applications.

Statement of Significance

One of the key aspects of tissue engineering is controlling cell behavior using hierarchical structures. Compared to 2D surfaces, fibers are an important class of materials, which can emulate the native ECM architecture of tissues. Despite the importance of both fiber surface topography and alignment to direct growing neurons, the current state of the art did not yet study the synergy between both scales of guidance. To achieve this, we established a solvent assisted spinning process to combine these two crucial features and control neuron growth, alignment, and branching. Rational design of new platforms for various tissue engineering and drug discovery applications can benefit from such information as it allows for fabrication of functional materials, which selectively influence neurite behavior.

1. Introduction

The extracellular matrix (ECM) of the nervous system is a complex 3-dimensional (3D) microenvironment with a large spectrum of topographical features, affecting the organization and growth

* Corresponding author at: DWI-Leibniz Institute for Interactive Materials, Aachen 52074, Germany.
E-mail address: delaporte@dwi.rwth-aachen.de (L. De Laporte).

https://doi.org/10.1016/j.actbio.2020.07.014

of the developing nervous system. During neuronal development, growth cones, located at the leading edges of axons, play the important role of detecting and responding to environmental cues that direct pathfinding [1,2]. There are four main mechanisms contributing in guiding growth cones: contact attraction, chemoattraction, contact repulsion, and chemorepulsion [2]. During the past decades, tremendous work has been dedicated to study different chemorepelling and -attracting guidance cues [1]. For example, studies on axon guidance mechanisms of *C. elegans*, Drosophila, and vertebrates have demonstrated the ability of netrins to function as both chemo attractant and -repellent secreted proteins [3]. In addition to the ECM biochemical cues, neuronal growth is also affected by the physical parameters of the cell 3D microenvironment, i.e. contact repulsions and attractions. There is an increasing evidence that a surface topography at variable micro- and nanoscale can influence different cellular behaviors, such as migration, growth rate, and differentiation [4]. This might be due to the scale of multiple anatomical factors and their subcellular features in the nervous system. For instance, filopodia, the smallest units of growth cones, possess finger-like structures (100–300 nm), which contribute directly to neuronal guidance at the nanoscale. At the microscale, growth cones, with the area of approximately 1–50 μm^2 depending on cell and growth cone type [5], are connected to the cell body by axons with diameters in the range of 0.1–10 μm [6,7]. Substrates with nano- and microscale anisotropic topographical features have shown to affect nerve cell unidirectional growth and stem cell differentiation [8]. Previous studies on human embryonic stem cells (hESCs) cultured on microgrooved surfaces showed that neuronal differentiation and groove height were inversely proportional with an increase in neuronal growth when cultured on a surface with 2 μm ridges compared to a flat surface [9]. At the nanoscale level, a 350 nm ridge pattern demonstrated effective and rapid differentiation of hESCs into a neuronal lineage without using any differentiation-inducing agent [10]. Although the vast majority of studies reported the alignment of neurites parallel to grooves on patterned substrates, perpendicular guidance has been observed as well. Neurites encountering the edge of a groove or a linear topographical discontinuity have to make a decision to either cross or follow it. While this choice is highly dependent on both the pattern dimensions and the cell type, certain cellular types resist following grooves that are too closely spaced or too deep, and instead bridge the gap to reach the adjacent features, resulting in extension perpendicular to the orientation of the grooves. In particular, various types of central nervous system neuroblasts have shown perpendicular growth to micro grooves with depths of 300–800 nm and a width of 1 μm [11,12].

In addition, few studies have shown that the electrospun fiber density (i.e. number of fibers in a certain area) also influences neuronal alignment. Scaffolds with high fiber density (> 1500 fibers/mm) led to perpendicular neurite extension on fibers lacking a laminin (LN) coating [13]. In the absence of LN, neurites tend to form bundles due to their poor interaction with the fibers and start to grasp and pull the fibers along the perpendicular direction as a rescue mechanism. In the case of neurite branching, it has been shown that neurites on aligned fibers exhibit little to no branching in contrast to randomly oriented fibers [14]. However, neurite branching in response to topographical cues, and more specifically, fiber surface topographies has not yet been studied.

While different techniques have been established to fabricate substrates with nano- and micron-scale topographies, most of them are prone to high costs, long preparation times, and small-size areas. Moreover, conventional surface patterning techniques, such as soft lithography [15] and temperature imprinting [16], are often 2D or lack the 3D fibrillar structure of the native ECM [17]. Recently, other techniques, such as the plasmonic photopatterning of aerogels, have been suggested for surface patterning of 3D scaffolds, and are currently under development [18]. Therefore, polymeric fibers have recently become very popular materials for harnessing and studying specific cell behaviors *in vitro* to solve tissue engineering challenges by a closer approximation of tissue dimensionality via pseudo 3D or 2.5D environments. While one of the most versatile and widely applied methods to fabricate nanofibrous mats is solution electrospinning (SES), the applied voltage induces the uncontrolled motion of the charged polymer jet [19]. This subsequently leads to a tightly packed mesh with small pore sizes hindering cell infiltration and vascularization. Moreover, the uncontrolled distance between fibers further limits studying cell−single fiber interactions as cells are in contact with multiple fibers at once in a 2D manner [20]. Even though it has been shown that certain surface topographies (e.g. porous, grooves) can lead to higher neurite alignment or longer extensions [21,22], this effect has not been investigated with respect to the distance between anisotropic cues.

We recently demonstrated the ability of the solvent assisted spinning (SAS) technique to continuously produce microfibers with distinct surface topographies [23]. By altering the applied solvent properties, microfibers with smooth, grooved, and porous surface topographies were produced in the absence of high voltage. While the microscale topographical cues, provided by aligned fibers themselves, results in cell guidance and polarized morphology, nano- to microscale morphological features at the fiber surfaces affect cell mechanotransduction [23]. Importantly, SAS enables the control of the inter-fiber distance (IFD) during the fabrication process. This provides a unique platform to study the role of fibrous physical guidance, recapitulating the natural ECM topographical features, in nerve guidance and regeneration. In this study, SAS technique is used to study the effect of the combination of fiber alignment, distance, and topography on contact guidance to influence neurite behavior of primary neurons, dissociated from chick embryonic DRGs, such as its growth extension, linear growth, and branching.

2. Materials and methods

2.1. SAS fibers fabrication and characterization

All chemicals are used as received without any further purification. SAS fibers are produced as previously described [23]. Briefly, polycaprolactone (PCL) with an average molecular weight of 80 kDa (Sigma-Aldrich, Germany) is dissolved in the binary solvent systems of chloroform (CF) - acetic acid (AA) (50–50, v/v), CF - dichloromethane (DCM) (75–25, v/v) or CF- dimethylformamide (DMF) (75–25, v/v), for smooth, porous, or grooved surface topography, respectively. To achieve the desired fiber diameter, a polymer concentration of 17 wt% (for smooth fibers) or 15 wt% (for porous and grooved fibers) is used. Syringes (1 mL) are filled with the prepared solution and mounted on a programmable syringe pump (Aladdin, WPI) positioned above a rotating collector at a vertical distance of 5–10 cm. The solution feed rate is varied between 50 and 150 μL/hr. As the solution is pushed through the needle (21 G), it forms a hemispherical shape at the tip, which is manually drawn towards the rotating collector (square glass = 1 × 1 cm) that collects aligned microfibers with specific topographies depending on the applied solvent system. The rotational speed of the collector is controlled via a digital speed controller and is set at 50 rpm. The rotating collector is placed on top of a translational linear stage with adjustable speed (V_T) to collect fibers at an IFD of 10, 30, 50, or 100 μm (V_T = 1, 3, 5, or 10 mm/min, respectively). All experiments are performed at room conditions with a temperature of 22–25 °C and a relative humidity of 42–45%. Before collecting the fibers, the glass surfaces are coated with a thin

layer of polydimethylsiloxane (PDMS) to ensure fiber immobilization upon depositing on the surface. To do this, a PDMS solution is prepared by mixing the crosslinker and base elastomer at a ratio of 1:40 (Sylgard 184, Dow Corning). Using a viscous pipette, 9 µl of the PDMS solution is deposited on the surface of a glass slide (1 × 1 cm), which is placed on a spin coater (Novocontrol, Germany). The spin coater is connected to a vacuum pump to maintain the glass slide in the center of the device during spinning. The spinning time, speed, and ramp are adjusted to T-2.50 (~ 3 min), S-3.50 (3000 rpm), R-0, respectively. PDMS coated glass slides are incubated at 80 °C overnight to cure the PDMS. Due to the applied mixing ratio (1:40), the resulting PDMS layer exhibits an adhesive property, which can be used to immobilized fibers on the surface of glass slides.

2.2. Cell culture and immunostaining

For cell seeding, samples are UV sterilized for one hour, incubated at 37 °C in a fibronectin (FN, 10 µg/ml, Sigma-Aldrich, Germany) solution overnight, and washed 3 times with sterile PBS prior to cell seeding. This is to ensure a FN coating across the entire surface so that the observed results are mainly due to the physical properties of substrates and not their chemical characteristics.

DRGs are isolated from E9–10 chick embryos as previously reported [24]. DRGs are harvested and stored in HBSS (Hank's buffered saline solution, Life Technologies), prior to placement on top of the fibers. To ensure attachment of the DRGs (>200 µm) to fibers and avoid their floating after adding media, a small droplet (10 µL) of fibrin hydrogel is added on top. Fibrin is chosen as neurites are known to grow through this gel [24] and can exit the gel to continue their growth on the fibers. For single nerve cells experiments, DRGs are dissociated by incubating them for 30 min at 37 °C in 10X trypsin (Sigma-Aldrich, Germany), followed by trituration with fire-polished glass Pasteur pipettes to dissociate the ganglia. Neuronal cells are separated by panning for 1 h at 37 °C. 1 mL of a suspension with single neuron cells (100,000 cells/mL) is prepared in Dulbecco's Modified Eagle Medium (DMEM, Lonza, Germany), supplemented with 10% fetal bovine serum, 1% antibiotics/antimycotics, 10 ng/mL nerve growth factor (NGF, PeproTech, Germany), and placed on top of the fibers. Both DRGs and single nerve cells are cultivated for 7 days at 37 °C, 5% CO_2, and 95% humidity. To study the neurite growth rate form DRGs, they are cultured for 1, 4, and 7 days *in vitro* (DIV).

The immunostaining is performed as previously described [24]. Briefly, samples are fixed with 4% paraformaldehyde (AppliChem, Germany), permeabilized with 0.1% Triton X-100 (Sigma-Aldrich, Germany), and blocked with 4 wt% bovine serum albumin (BSA, Sigma-Aldrich, Germany) in PBS. Neurons are stained with neurotubulin antibody (1:250 TUJ1 monoclonal antibody mouse-derived, Sigma-Aldrich, Germany), followed by a secondary fluorescent antibody (Alexa Fluor 488 anti-rabbit or Alexa Fluor 633 anti-mouse (Thermo Fisher Scientific, 1:100)). The nuclei are stained with 4′,6-diamidino-2-phenylindole (DAPI, Biolegend, Germany) at the concentration of 2% (v/v) in PBS.

2.3. Image analysis

The surface topography and the diameter of the fibers are analyzed using field emission scanning electron microscopy (FESEM-Hitachi S4800, Japan). Prior to imaging, fibers are sputter coated with gold-palladium. ImageJ (1.51 W, NIH, USA) software is used to characterized fiber alignment, diameter, and their topography. In order to evaluate the effect of fiber surface morphology on neurite orientation and growth, the fluorescent images of stained cells are imported to ImageJ software as "binary" images. The OrientationJ Distribution function is applied, using a Gaussian window of 1 pixel and the Fourier Gradient function.

Alignment of the neurites in relation to the oriented fibers is evaluated according to the distribution of angles relative to the vertical plane (fibers). Neurites from immunostained images are traced in ImageJ for each condition. The orientation angle relative to the vertical plane is plotted for all the conditions. A neurite extension is considered aligned when the deviation from the fiber alignment is less than 15°. The percentage of neurites with a deviation of more than 15° is plotted for each condition. Cell migration is calculated by nucleus staining. The migration distance is measured as the width of a rectangle drawn from the edge of the DRG body to contain all neurite extension in the direction of the fibers (Fig. 3, A).

2.4. Statistical analysis

Statistical analysis is performed with OriginPro 2016 G. A one-way ANOVA is executed with post-hoc Tukey comparison for evaluation of statistical significance between groups ($*p < 0.05$). Data are shown as mean average with error bars indicating the standard deviation. Not significant differences are defined by "n.s.". All image analysis of single neurons is performed at n (≥40). Neurite extension analysis is performed for n (≥ 100).

3. Results

3.1. SAS fibers scaffolds

Using SAS, highly aligned PCL fibers with an average diameter of ~ 10 µm are spun in the absence of an electric field (Fig. 1, A). Fibers with distinct surface topographies are produced by altering solvent properties (i.e. volatility and solubility). Smooth, porous, or grooved fibers are spun from PCL dissolved in the binary solvent systems of CF - AA (50–50, v/v), CF - DCM (75–25, v/v) and CF-DMF (75–25, v/v), respectively (Fig. 1, B).

Fibers are collected on cover glass slides with 10, 30, 50, and 100 µm IFDs. To ensure fiber stability during the *in vitro* experiments, the surfaces of the cover glasses are coated with a thin PDMS layer. The ratio between the curing agent and resin is specifically modified to result in a sticky surface after a complete curing process. This enables a successful immobilization of a single layer of fibers on the glass surface without fibers sinking completely into the PDMS layer (**Fig. S1, Supporting Information**). While all fibers are aligned unidirectionally at the macron-scale, porous and grooved fibers provide a secondary surface topography at the micro- and nanoscale.

3.2. DRG growth on SAS fibers with different surface topography

To study the effect of fiber surface topography on neurite extension, full DRGs are initially cultured on aligned fibers collected at a high density (IFD = 0 µm). It is observed that neurite extension is similar for smooth (1.6 ± 0.5 mm) and porous (1.7 ± 0.4 mm) fibers, while significantly longer neurites extend from DRGs on grooved fibers (2.3 ± 0.4 mm) (Fig. 2, B). Interestingly, in the case of smooth and porous topographies, some neurites tend to grow initially in a radial direction before turning their growth parallel to the fiber alignment. This results in final DRG surface coverage with slightly smaller aspect ratios on smooth and porous fibers (3 ± 1) compared to grooved fibers (4 ± 1), yet not statistically significant (Fig. 2, C).

Accordingly, a higher DRG growth rate is observed on grooved fibers compared to smooth and porous fibers. To gain more insight into this, smooth, porous, and grooved fibers are collected on a

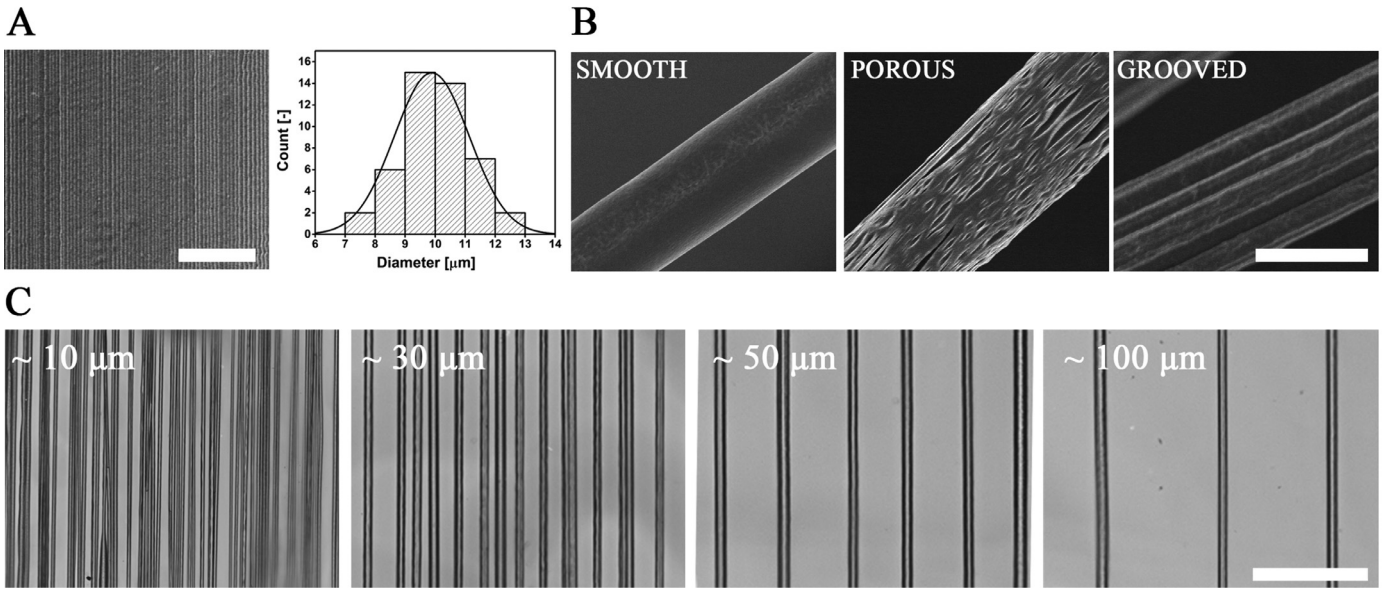

Fig. 1. The ability of SAS in producing highly aligned fibers with a distinct surface topography and IFD. Highly aligned fibers with an average diameter of 10 ± 1 µm are collected on a low speed (50 rpm) rotating drum (A). Scale bar is 500 µm. By changing the solvent system, smooth (CF-AA/50–50), porous (CF-DCM/75–25), and grooved (CF-DMF/75–25) fibers are achieved (B). Scale bar is 10 µm. Controlling the linear transition of a rotating drum allows for adjusting the IFD when using SAS (C). Scale bar is 100 µm. Fig. 1A and 1C demonstrate typical fiber alignment and spacing regardless of their surface topography.

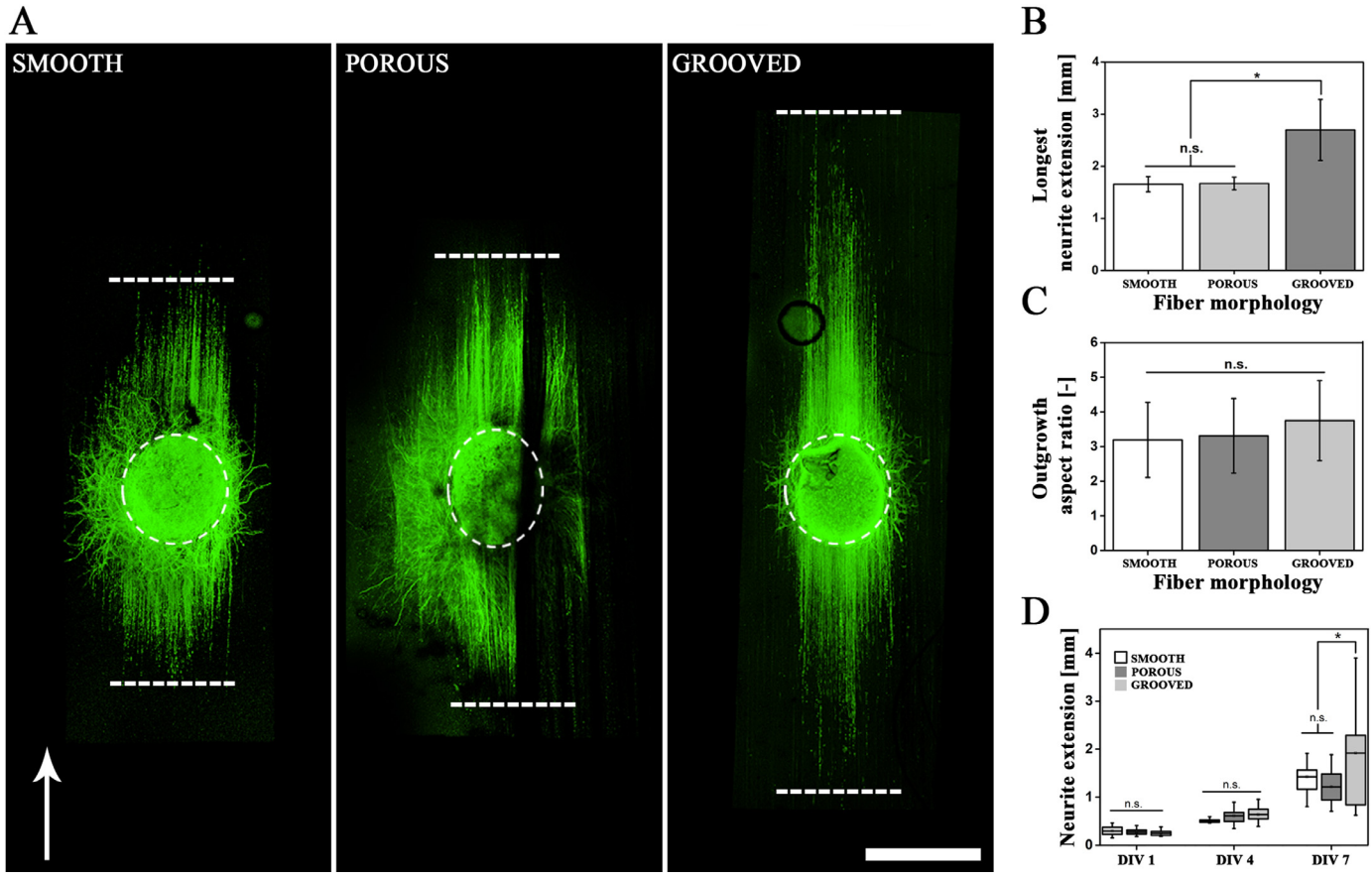

Fig. 2. Effect of fiber surface topography on DRG growth. DRG extension (green: ß tubulin) on SAS fibers exhibiting smooth, porous, and grooved topography (A). Grooved fibers demonstrate a significantly longer neurite extension compared to smooth and porous fibers after DIV 7 (B). Effect of fibers surface topography on DRG surface area aspect ratio after DIV 7 (C). Neurite extension length from DRGs on fibers after DIV 1, DIV 4, and DIV 7 (D). Scale bar is 1 mm. The white arrow shows fiber direction.

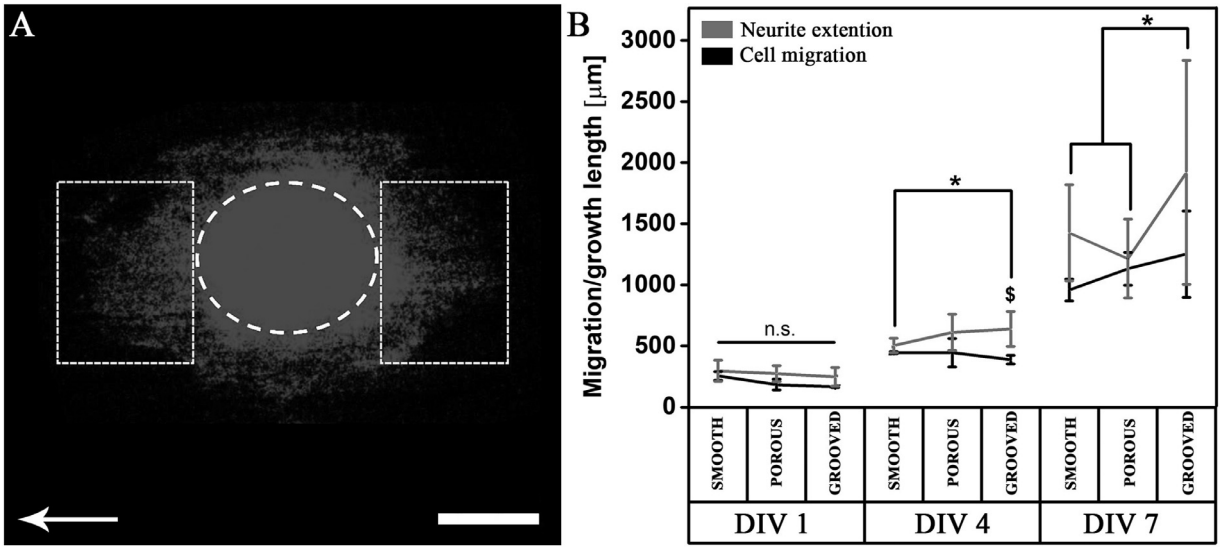

Fig. 3. A representative image of cell migration distance based on nucleus staining. The distance is measured as the width of a rectangle drawn from the edge of the DRG body to contain all cells grown in the direction of the fibers (A). Scale bar is 500 μm. Migration (in case of supporting cells) and outgrowth length (in case of neurites) are compared at 1, 4, and 7 DIV for smooth, porous, and grooved fibers (B). The white arrow shows fiber direction. Difference between neurite extension and cell migration is marked by $. Difference between neurite extension within each group is marked by *.

cover glass slide and DRGs are cultured for 1, 4, and 7 DIV prior to fixation and imaging. At time points 4 and 7 DIVs, neurites have sufficient time to extend out of the DRG. In addition, neurite extension is measured at 1 DIV, as neurites already start emerging from the DRG body at this early time point in culture. While the neurite length is similar for all fibers at DIV 1 and DIV 4, grooved fibers show a significant increase in length (1919 ± 916 μm) compared to smooth (1425 ± 394 μm) and porous (1215 ± 322 μm) fibers at DIV 7. When comparing DIV 7 and DIV 1, fibers with grooved surface topography induce the highest growth rate (~ 7-fold increase in length) followed by smooth and porous (~ 4-fold increase in length) fibers (Fig. 2, D).

As DRGs contain glial cells and Schwann cells (SCs) besides primary sensory neurons [25], the migration rate of these supporting cells on SAS fibers is analyzed via DAPI nuclei staining (Fig. 3, A). Comparing the migration distance of these cells and neurite extension, neurites slightly surpass the migrating cells. Neurite elongation is faster than cell migration at 1, 4, and 7 DIV for all fiber surface topographies, while a significantly longer neurite extension (638 ± 142 μm) is observed on grooved fibers compared to the overall cell migration distance (387 ± 35 μm) at DIV 4, in contrast to fibers with smooth or porous topography (Fig. 3, B).

3.3. Single neuron growth on SAS fibers with different topography and IFD

Single cells from dissociated DRGs are grown on coated glass slides without any fibers (**Fig. S2, Supporting Information**), or on top of fibers with different surface topographies at four specific IFDs (10, 30, 50, and 100 μm) (Fig. 1, C). Despite their surface topographies, increasing IFD results in less oriented neurite extensions (Fig. 4, A). Qualitative observations are further confirmed by analyzing the deviation of the neurite orientation angle relative to a vertical plane representing fiber alignment. Neurite extension is considered aligned when the deviation of angle is less than 15°, as previously described [26-28]. While at 10 and 30 μm IFDs, there is no significant difference between surface topographies, the deviation of angle is significantly lower for grooved fibers compared to smooth and porous fibers at IFD = 100 μm, and to porous fibers at IFD = 50 μm (Fig. 4, B). Accordingly, grooved fibers promote a higher percentage of aligned neurite extensions, compensating the increase in IFD (Fig. 4, C). Maximum alignment is, therefore, achieved on grooved fibers, with more than 90% of the neurite extensions demonstrating deviation angle lower than 15° at IFD 10, 30 and 50 μm, and ~ 70% of the neurites at IFD 100 μm. In contrast, only ~ 70% and ~ 50% of total neurites show alignment on porous fibers at an IFD of 50 and 100 μm, respectively. Strikingly, the percentage of aligned neurite extensions on grooved fibers at a large IFD of 50 μm (86%) is higher than those on porous fibers with the smallest IFD of 10 μm (83%). The significantly lower deviation of neurite angle from fiber orientation at an IFD of 100 for grooved fibers versus smooth and porous fibers demonstrates that axons growing in between the fibers are more aligned in the case of grooved fibers. This implies that once a neurite leaves a fiber, it may have some kind of memory installed by the micron-scale grooves.

The interaction of neurites with fibers is further evaluated by measuring the neurite length attached to fibers, the percentage of fiber crossing neurons, and the number of neuron branches (Fig. 5, A). As shown in Fig. 5, B, grooved fibers separated by an IFD of 30 μm promote the longest neurite extension attached to fibers compared to any other conditions. Interestingly, while grooved fibers enable longer neurite extension on the fibers at IFD of 10 and 30 μm, at larger IFDs, i.e. 50 and 100 μm, the difference between smooth and grooved surface topographies is less pronounced. This is interesting as in Fig. 4, B, neurites are significantly more aligned at an IFD of 100 for grooved fibers versus smooth and porous fibers.

To gain more insight on the effect of fiber surface topography and IFD on neuronal growth, the percentage of cells with extensions crossing over fibers and the number of branches are investigated (Fig. 5, A). An enhanced number of neurites crossing the fibers is shown for increasing IFD (Fig. 5, C). For example, at low IFD of 10 μm, porous fibers lead to more fiber crossing, while at a larger IFD of 50 μm, grooved fibers seem to reduce fiber crossing. At the largest IFD of 100 μm, the distance between the fibers dominates and the topography does not affect fiber crossing anymore. When comparing the number of branches, neurons do not show any significant differences at low IFDs (i.e. 10 and 30 μm), while at higher IFDs (i.e. 50 and 100 μm) they tend to significantly increase their branching activity for all topographies (Fig. 5, D).

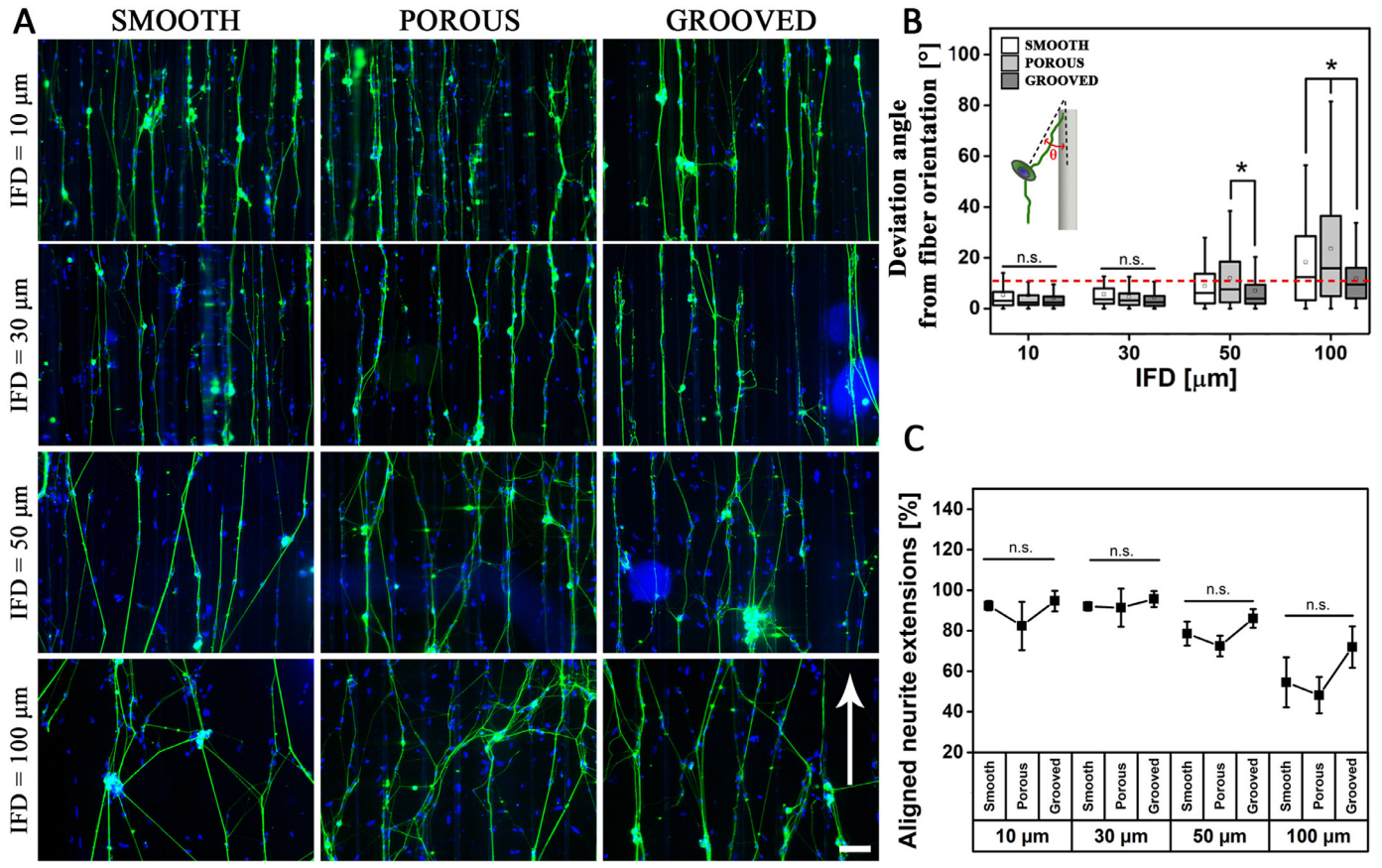

Fig. 4. Effect of combination of topography and IFD of SAS fibers on unidirectional nerve growth. Neurite extensions of single neurons (green: ß tubulin) on fibers exhibiting smooth, porous, or grooved topography at different IFDs (10, 30, 50, or 100 µm) (A). The white arrow shows fiber direction. Scale bar is 100 µm. Deviation of the orientation angle (schematically shown in the graph) measured for neurite extensions on smooth, porous, and grooved topography at different IFDs ($n \geq 100$) (B). A neurite extension is considered aligned when the deviation of angle is less than 15° (marked with the red dashed line) in (B). Percentage of aligned neurite extensions depending on the fiber surface topography and IFD (C). (For interpretation of the references to colour in this figure legend, the reader is referred to the web version of this article.)

When comparing the above mentioned observations with neurite and total cell surface area density, a grooved topography leads to a higher neurite density at low IFD (10 µm) but when the fiber distance increases, this trend is observed on the porous fibers with reduced neurite density on grooved fibers (**Fig. S3, A, Supporting Information**). This may be explained by the fact that both neurites on and in between the fibers are more aligned and thus grow in a straight path, resulting in lower densities, which might be associated to the topographic memory. The higher branching on porous fibers at high IFD could further contribute to these higher neurite densities at large IFDs (≥ 30 µm). Interestingly, similar trends are seen for total cell density, including the supportive cells, like SCs (dissociated from the DRGs), where higher numbers of cells are observed at large IDFs and porous fibers seem to result in higher cell proliferation (**Fig. S3, B, Supporting Information**). Based on these similarities, it is highly likely that the produced bioactive factors from supporting cells enhance neurite growth.

4. Discussion

The SAS technique is advantageous for fiber fabrication with distinct surface topography and defined IFDs, which is otherwise difficult to achieve with conventional SES method. The mechanism of the formation of topographies has been elucidated in our previous publication [23]. Briefly, depending on the solvent property, thermally or non-solvent induced phase separation takes place during solvent evaporation from the surface of the polymeric jet, which results in a specific void solidification pattern as the fiber is being pulled by the rotating drum, and therefore in a smooth, porous, or grooved topography. This is particularly an important feature of SAS compared to SES as the latter technique is associated with a high whipping motion caused by the polymer surface charge [23]. Based on our previous study, porous fibers possess pores with a length and width of ~ 2 µm and ~ 0.3 µm, respectively, while the average ridge width of grooved fibers is ~ 1.5 µm [23]. As a result, we obtain surfaces with hierarchical topographical features similar to axon sizes providing a unique contact guidance construct at 2.5D.

The observed linear neurite extension at high density (IFD = 0 µm) is in agreement with previous studies, in which linear neurite extensions were observed on aligned electrospun fibers compared to randomly oriented fibers [29]. When studying the effect of fiber physical properties (i.e. surface roughness or topography), macrophages and astrocytes exhibited a more elongated morphology on smooth fibers compared to fibers with porous surface topography [30,31]. In the case of fibroblasts cultured on the fibers tested in this report, no difference in cell elongation is observed between smooth an porous fibers but cell portrayed a more spiky morphology on porous fibers with higher nuclear yes-associated protein (YAP) levels [23]. On the other hand, previous reports demonstrated that smooth fibers resulted in longer neurite extension from DRGs compared to porous fibers, whereas no significant difference was observed when both fibers were coated with LN [32].

The larger DRG aspect ratio on grooved fibers compared to smooth and porous fibers is likely due to the initial radial growth

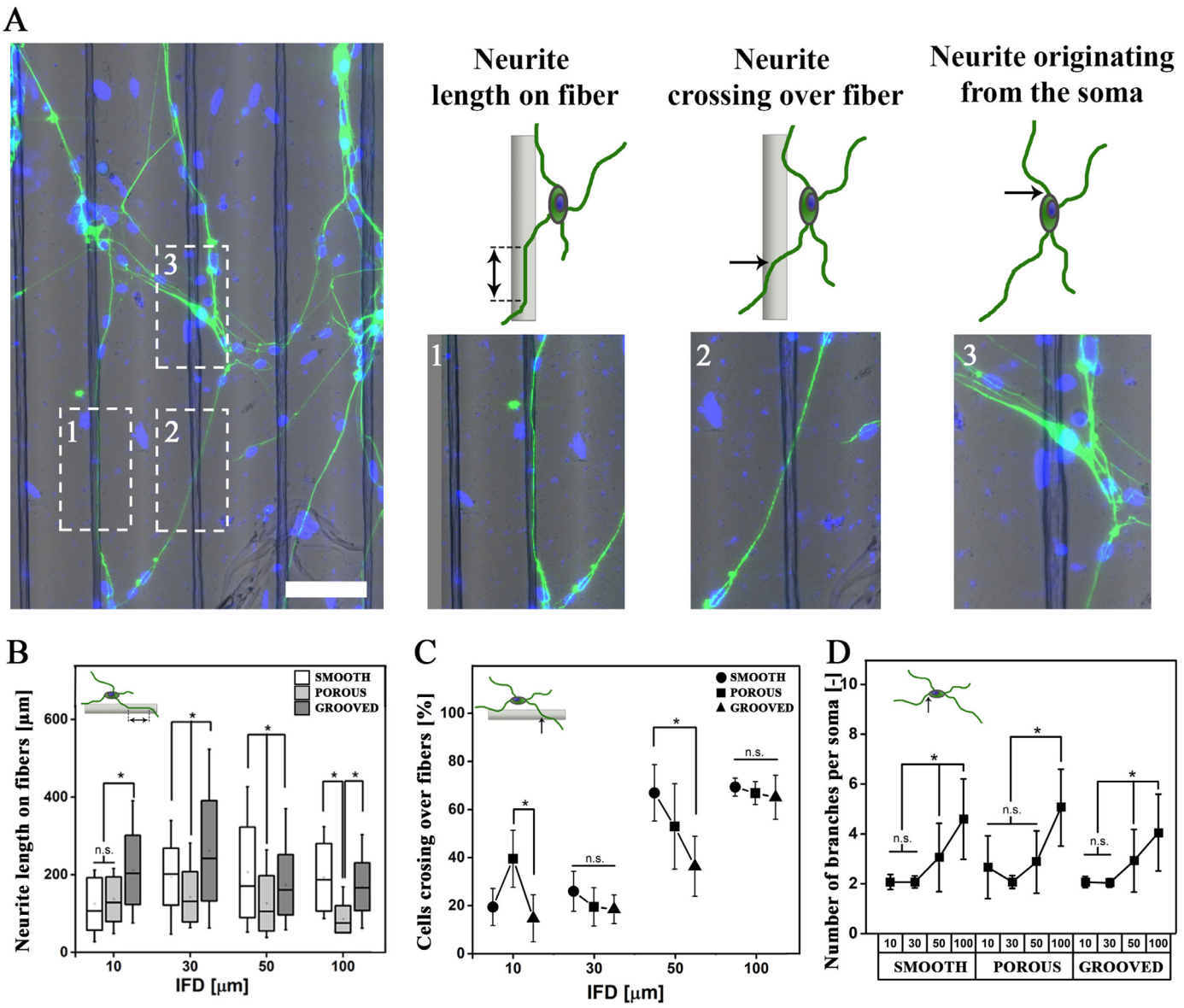

Fig. 5. A schematic representation of neurite morphometric parameters. Neurite length on fiber (A1), neurite crossing over fiber (A2), and neurite branching originating from the soma (A3). Scale bar is 50 µm. Neurite length on fibers (B), percentage of cells crossing over fibers (C), and average number of branches per soma (D) are measured depending on the fiber surface topography and IFD. (For interpretation of the references to colour in this figure legend, the reader is referred to the web version of this article.)

of DRGs on smooth and porous fibers. Previously, it has been shown that neurite extension from DRGs cultured on aligned smooth electrospun fibers first extended randomly in all directions, after which they would come into contact with the fibers and change their growth direction to follow the fiber alignment [33]. Here, the micron-scale ridges on the surface of grooved fibers restrict this initial lateral extension of neurites and consolidate neurite growth into parallel arrays following the long axis of fibers immediately. Essentially, each ridge likely orients neurite extension in a similar manner to individual fibers with smaller diameters as the groove size is especially suited for guiding axons towards their target site. Considering misdirected axonal growth as one of the main challenges in nerve regeneration, hindering functional recovery, the restoration of native structural organization is particularly important [34,35].

Grooved fibers seem to induce a higher DRG growth rate, parallel to the direction of fibers, compared to smooth and porous fibers. This may be due to the fact that smooth and porous fibers do not necessarily provide restrictions to the neurites to grow only along fibers. On the contrary, grooves provide an additional contact guidance along the alignment direction, restricting neurite growth, and therefore supporting a faster rate along the fibers. A previous study demonstrated that larger growth cones with significant lateral expansion of lamellipodia and filopodia have a negative effect on neurite growth and result in a decreased growth rate [36]. It is believed that this is due to the lack of efficient sensing of environmental cues, which results in a poor alignment between the central domain of the growth cone and the direction of advancement. By changing a 2D culture environment (poly-L-lysine substrate) to a fibrous 3D environment (collagen gel), a morphologically different growth cone and faster growth rate were observed, which was attributed to the presence of micron-scale topographical cues from the collagen fibers that were sensed and responded to by the growth cones. Taking into consideration the slow human axon regeneration rate (~ 2 mm/day) [37], which can lead to several months of healing process in case of significant injuries,

grooved SAS fibers can provide these micro-physical contact cues and could, therefore, be used to develop new types of regenerative biomaterials enabling a faster axonal growth rate.

While several biochemical approaches, such as the addition of growth factors [38], fibrin [39], and collagen [40] to a scaffold have shown to enhance neurite growth, the presence of SCs also demonstrated an improved neuronal growth likely due to their ability to express neurite promoting factors, such as neurotrophins [35,41]. A previous study has shown that SCs migrating ahead of neurite outgrowth may be establishing a pathway for neurite extension on uncoated smooth fibers, whereas on fibers coated with LN or FN, the neurites grew past the SCs suggesting that at the presence of ECM support is sufficient to promote neurite growth [42]. In this report, significantly longer neurite extension than the cell migration distance on grooved fibers suggests that the micron-scale surface ridges promote longer neurite extension independent of supporting cell migration, as the migration distance of the supporting cells does not increase on the grooved fibers.

Besides surface topography, the distance between contact guiding elements also influences the neurite decision-making process. For example, an increase in microfiber (diameter ~ 2.5 μm) density (i.e. by increasing fiber collection time during SES) has demonstrated a reduction in neurite linear pathfinding, likely due to the ability of growth cones to migrate to adjacent fibers, resulting in neurites steering away from the linear pathway. Despite the importance of IFD, conventional SES fiber fabrication techniques are limited as the fiber density and periodicity can only be altered by changing the collection time, therefore, also leading to multiple fiber layers on top of each other. In order to control fiber density in a monolayer manner, and thus the IFD, while providing different topographies in a precise and reproducible manner, SAS provides unique properties. This is particularly important to study for the design new types of scaffolds for nerve regeneration as growth cones experience a large spectrum of topographies *in vivo* [13,43].

To elucidate these nerve-material interactions, single cells from dissociated DRGs are grown on top of fibers with different IFDs. Depending on the IFDs, some cells land on the glass slide in between the fibers following cell seeding. After encountering a fiber when coming from the lower glass surface, the growth cone of the neurite moves along the fiber for some distance. Depending on the fiber surface topography, the neuronal process on top of fibers will decide to either grow along the fiber or to cross the fiber and potentially bifurcate into their daughter branches. When leaving the fiber again, neurites grow more aligned after having encountered a grooved fiber. Such type of topographical memory might be similar to what has been observed in the case of stem cell mechanical memory. For instance, neuronal stem cells (NSCs) can "remember" past topographies depending on the exposure time to these topographies. When in contact with a nano wrinkle topography for longer times (5 days), NSCs retained their orientation even after removing the cells from the topography, in contrast to NSCs exposed for a shorter time (1 and 3 days) [44]. Topographical memory is likely associated with nuclear YAP translocation, as this is one of the mechano-sensitive pathways through which cells undergo changes in gene expression, and has demonstrated to be affected by past culture conditions. Such memory effects have shown to remain for a long period of time. For example, after initially culturing human mesenchymal stem cells on a stiff substrate, YAP remains in the nucleus for 10 more days after the substrate was softened [45]. In addition, a recent study demonstrated the role of surface topography in nuclear YAP translocation in neuron-like cells, where higher YAP activation was observed in the nucleus of PC 12 cells when cultured on nanogroove surfaces compared to flat substrates [46]. On the other hand, nuclear YAP translocation has been linked to nucleus elongation [47], which can be caused by focal adhesion reorganization. Focal adhesions transmit mechanical signals from the extracellular environment to the nucleus and their orientation and size is highly affected by surface topography [48]. For example, mesenchymal-like cells, cultured on grooved surfaces, demonstrate restricted growth of focal adhesions within the topographical features, leading to their linear organization parallel to the ridges [49]. The same effect was observed in the case of PC 12 neuronal cells cultures on grooved surfaces [46], and for myosin growth in collagen matrices, with individual adhesions observed in the direction of local collagen fibers [50]. This is consistent with our previous finding, where fibroblast cells showed linear protrusion growth within the ridges of grooved fibers due to their underlying focal adhesion reorganization [23]. More pronounced vinculin expression (as a focal adhesion indicator) was observed in the periphery of cells when cultured on grooved and porous fibers, whereas smooth fibers mainly led to cytosol vinculin expression. In both cases, nuclear YAP was enhanced, with a significantly higher nuclear aspect ratio in the case of grooved fibers. Given the role of YAP expression in neural differentiation and morphology [46], it is likely that "topographical memory" is affected by internal forces inside the cells, created by focal adhesions and mediated by nuclear YAP translocation.

In addition to potential "topographical memory", the percentage of cells with extensions crossing over fibers is important information when designing new biomaterials, for example, for bridging the two ends of a nerve injury gap, as unidirectional growth of neurons parallel to the guidance elements is highly desired. Early studies have shown that the mere presence of physical constrains does not always result in unidirectional growth, as growth cones were able to span over several neighboring grooves and ridges [51]. For example, studies have shown an opposite relation between the depth of topographical cues and the frequency of crossing. Groove depths equal to or larger than 4.7 μm completely restrained hippocampal neurites from crossing over the ridges [51], similar to embryonic chick neurons in the case of 4 μm groove depths [52]. This suggests that unidirectional orientation depends on the microenvironment geometry, such as the number and frequency of pattern repeat, which emphasizes the importance of IFD and the interaction of neurites with fibers featuring different surface topographies in the active process of nerve cell decision-making.

Considering the average diameter of the fibers that are used within this study (diameter ~ 10 μm), one would expect that neurites extensions would always keep growing along the fibers once they encounter them instead of crossing them over. However, neurite crossing is shown to be modulated by the IFD with an increasing number of neurites crossing the fibers at increasing IFD (Fig. 5, C). This suggests that at lower IFDs, growth cones can sense the nearby aligned fibers, triggering them to maintain their path. Being exposed to both attractive and repulsive guidance in their microenvironment, cells decide to follow a fiber path or cross it and make a connection with cells on the other side. Neurite-neurite contact plays a crucial role in shaping individual neurites and their networks by providing an attractant gradient role for growth cones via many trans-Golgi vesicles at neurite intersections [53,54]. It is known that neurite intersections are enriched with trans-Golgi vesicles [55], which are trapped in clusters of the adhesion molecule N–CAM, and can produce an attractant gradient for growth cones [54]. This can result in axon reorientation as growth cones change their direction towards the attractant, which may explain why growth cones cross fibers when larger gradients originate due to neurite interactions. Therefore, at large IFDs, a neighboring neuron intersection might act as a stronger attractant gradient leading to more neurites crossing the fibers. In addition, due to higher neuron-neuron interactions compared to neuron-fiber interactions at larger IFD, neurites tend to form bundles and fasciculate more caused by the lack of sufficient guiding elements, independent of the topography (**Fig. S4, Supporting Information**). There-

fore, at high IFD, neurites growing along a fiber seem to exhibit a preferential attraction to their neighboring neurons rather than to keep their direction along a fiber. In addition, a porous topography seems to further decrease the ability of a neurite to follow the fiber. This reveals that neurite "decision-making" behavior on whether to cross a fiber or grow long is not only dependent on the IFD but also on the fiber surface topography, depending on the IFD. Likely, this is to enhance the probability of finding neighboring cells due to lack of sufficient contact guidance elements.

Increasing the IFD also promotes a higher number of branching. The morphology of dendritic trees and axonal organization influence the way neurons receive and process information and how neuronal circuits develop. This involves the control of branching, growth, and stabilization of the network by various intrinsic and extrinsic factors, such as soluble biomolecules and proteins, physical contact guidance in cell-material interactions, and contact-induced signaling of surface molecules [54]. Depending on these interaction states, neuronal patterns vary from isolated neurons with more branches before contact with these guiding cues to a more economical behavior with lower number of branches and longer neurites [56,57]. When comparing neurite and total cell density for the different topographies and IFDs, similar trends are observed. While it is not completely clear why the topographic effect is not visible for total cell density at low IFD (i.e. 10 µm), the results imply higher cell proliferation at large IFDs, thus in the space between the fibers, while porous fibers enhance cell division. Higher cell proliferation on porous fibers might be influenced by more adsorption of fibronectin on these fibers. Previously, an increase in surface roughness and porosity have shown to result in higher protein adsorption [58]. Taken together, the trends observed for different neurite behavior, such as following or crossing the fibers and neurite branching, and the convenient control of both the IFD and fiber topography by the SAS technique, displays a robust approach for a rational design of scaffolds for neural and other engineered tissues.

5. Conclusion

This study demonstrates the usage of SAS fibers to study the combinatorial effect of fiber surface topography and defined IFDs on neuronal growth, orientation, and branching for the first time. SAS enables controlling fiber surface topography (smooth, porous, grooved) by altering solvent properties while the IFD can be tuned reliably in the absence of an electric voltage in contrast to conventional SES fibers spinning techniques. While decreasing the IFD improves oriented growth, the maximum percentage of aligned neurite extension is observed on grooved fibers at an IFD of 30 µm. At larger IFDs, porous fibers demonstrate a higher number of branches origination from somas, likely due to the neurons' decision in exploring and connecting with neighboring neurons to enhance cell-cell interaction at the absence of sufficient guidance element. To achieve this, neurons also cross over fibers and are attracted by neurite intersections at higher IFD. Overall, grooved fibers enhance oriented neurite extension on and in between fibers, leading to a higher growth rate and compensating the neurites' need to cross fibers at an IFD of 50 µm. Compared to smooth and grooved fibers, porous fibers inhibit neurite growth attached to the fibers and less neurons grow in parallel with the fiber orientation. These results suggest how fiber surface topography can be used at certain IFDs to induce a specific cell decision. SAS provides a unique platform to perform such studies across different hierarchical scales in a reliable and reproducible manner. This is of great importance when designing new types of biomaterials for various nerve and other tissue engineering applications.

Author contributions

The manuscript was written through contributions of all authors. All authors have given approval to the final version of the manuscript.

Declaration of Competing Interest

The authors declare that they have no known competing financial interests or personal relationships that could have appeared to influence the work reported in this paper.

Acknowledgments

This work was supported by the funding from the European Research Council (ERC) under the European Union's Horizon 2020 research and innovation program (ANISOGEL, grant agreement No 637853). This work was performed in part at the Center for Chemical Polymer Technology CPT, which was supported by the EU and the federal state of North Rhine-Westphalia (grant EFRE 30 00 883 02). Financial support is acknowledged from the European Commission (EUSMI, 731019). We gratefully acknowledge funding from the Leibniz Senate Competition Committee (SAW) under the Professorinnenprogramm (SAW-2017-PB62: BioMat).

Supplementary materials

Supplementary material associated with this article can be found, in the online version, at 10.1016/j.actbio.2020.07.014.

References

[1] A.B. Huber, A.L. Kolodkin, D.D. Ginty, J.F. Cloutier, Signaling at the growth cone: ligand-receptor complexes and the control of axon growth and guidance, Annu. Rev. Neurosci. 26 (2003) 509–563.
[2] M. Tessier-Lavigne, C.S. Goodman, The molecular biology of axon guidance, Science 274 (5290) (1996) 1123–1133.
[3] A. Chisholm, M. Tessier-Lavigne, Conservation and divergence of axon guidance mechanisms, Curr. Opin. Neurobiol. 9 (5) (1999) 603–615.
[4] G. Charras, E. Sahai, Physical influences of the extracellular environment on cell migration, Nat. Rev. Mol. Cell Biol. 15 (2014) 813.
[5] K.W. Tosney, L.T. Landmesser, Growth cone morphology and trajectory in the lumbosacral region of the chick embryo, J. Neurosci 5 (9) (1985) 2345–2358.
[6] J.A. Perge, J.E. Niven, E. Mugnaini, V. Balasubramanian, P. Sterling, Why do axons differ in caliber? J. Neurosci. Offic. J. Soc. Neurosci. 32 (2) (2012) 626–638.
[7] D. Liewald, R. Miller, N. Logothetis, H.J. Wagner, A. Schuz, Distribution of axon diameters in cortical white matter: an electron-microscopic study on three human brains and a macaque, Biol. Cybern 108 (5) (2014) 541–557.
[8] M.F. Griffin, P.E. Butler, A.M. Seifalian, D.M. Kalaskar, Control of stem cell fate by engineering their micro and nanoenvironment, World J. Stem Cells 7 (1) (2015) 37–50.
[9] D. Lu, C.S. Chen, C.S. Lai, S. Soni, T. Lam, C. Le, E.Y. Chen, T. Nguyen, W.C. Chin, Microgrooved surface modulates neuron differentiation in human embryonic stem cells, Methods Mol. Biol. 1307 (2016) 281–287.
[10] M.R. Lee, K.W. Kwon, H. Jung, H.N. Kim, K.Y. Suh, K. Kim, K.-S. Kim, Direct differentiation of human embryonic stem cells into selective neurons on nanoscale ridge/groove pattern arrays, Biomaterials 31 (15) (2010) 4360–4366.
[11] I. Nagata, A. Kawana, N. Nakatsuji, Perpendicular contact guidance of CNS neuroblasts on artificial microstructures, Development 117 (1) (1993) 401–408.
[12] I. Nagata, N. Nakatsuji, Rodent CNS neuroblasts exhibit both perpendicular and parallel contact guidance on the aligned parallel neurite bundle, Development 112 (2) (1991) 581.
[13] J. Xie, W. Liu, M.R. MacEwan, P.C. Bridgman, Y. Xia, Neurite Outgrowth on Electrospun Nanofibers with Uniaxial Alignment: the Effects of Fiber Density, Surface Coating, and Supporting Substrate, ACS Nano 8 (2) (2014) 1878–1885.
[14] S. Patel, K. Kurpinski, R. Quigley, H. Gao, B.S. Hsiao, M.-M. Poo, S. Li, Bioactive nanofibers: synergistic effects of nanotopography and chemical signaling on cell guidance, Nano Lett. 7 (7) (2007) 2122–2128.
[15] K.T.M. Tran, T.D. Nguyen, Lithography-based methods to manufacture biomaterials at small scales, J. Sci. Adv. Mater. Dev. 2 (1) (2017) 1–14.
[16] A. Nandakumar, R. Truckenmuller, M. Ahmed, F. Damanik, D.R. Santos, N. Auffermann, J. de Boer, P. Habibovic, C. van Blitterswijk, L. Moroni, A fast process for imprinting micro and nano patterns on electrospun fiber meshes at physiological temperatures, Small 9 (20) (2013) 3405–3409.
[17] Z. Nie, E. Kumacheva, Patterning surfaces with functional polymers, Nat Mater. 7 (4) (2008) 277–290.

[18] M. Rodriguez Sala, C. Peng, O. Skalli, F. Sabri, Tunable neuronal scaffold biomaterials through plasmonic photo-patterning of aerogels, MRS Commun. 9 (4) (2019) 1249–1255.
[19] W.E. Teo, S. Ramakrishna, A review on electrospinning design and nanofibre assemblies, Nanotechnology 17 (14) (2006) R89–R106.
[20] M. Simonet, O.D. Schneider, P. Neuenschwander, W.J. Stark, Ultraporous 3D polymer meshes by low-temperature electrospinning: use of ice crystals as a removable void template, Polymer Eng. Sci. 47 (12) (2007) 2020–2026.
[21] F. Yang, R. Murugan, S. Wang, S. Ramakrishna, Electrospinning of nano/micro scale poly(l-lactic acid) aligned fibers and their potential in neural tissue engineering, Biomaterials 26 (15) (2005) 2603–2610.
[22] F. Yang, R. Murugan, S. Wang, S. Ramakrishna, Electrospinning of nano/micro scale poly(L-lactic acid) aligned fibers and their potential in neural tissue engineering, Biomaterials 26 (15) (2005) 2603–2610.
[23] A. Omidinia Anarkoli, R. Rimal, Y. Chandorkar, D. Gehlen, J. Rose, K. Rahimi, T. Haraszti, L. De Laporte, Solvent induced nanotopographies of single microfibers regulate cell mechanotransduction, ACS Appl. Mater Interf. (2019).
[24] A. Omidinia-Anarkoli, S. Boesveld, U. Tuvshindorj, J.C. Rose, T. Haraszti, L. De Laporte, An injectable hybrid hydrogel with oriented short fibers induces unidirectional growth of functional nerve cells, Small 13 (36) (2017).
[25] V. Schaeffer, L. Meyer, C. Patte-Mensah, A.G. Mensah-Nyagan, Progress in dorsal root ganglion neurosteroidogenic activity: basic evidence and pathophysiological correlation, Prog. Neurobiol. 92 (1) (2010) 33–41.
[26] K.-.H. Nam, N. Jamilpour, E. Mfoumou, F.-.Y. Wang, D.D. Zhang, P.K. Wong, Probing mechanoregulation of neuronal differentiation by plasma lithography patterned elastomeric substrates, Sci. Rep. 4 (1) (2014) 6965.
[27] A. Ferrari, M. Cecchini, R. Degl Innocenti, F. Beltram, Directional PC12 cell migration along plastic nanotracks, IEEE Trans. Biomed. Eng. 56 (11 Pt 2) (2009) 2692–2696.
[28] M. Antman-Passig, O. Shefi, Remote magnetic orientation of 3D collagen hydrogels for directed neuronal regeneration, Nano Lett. (2016).
[29] N.J. Schaub, C.D. Johnson, B. Cooper, R.J. Gilbert, Electrospun Fibers for Spinal Cord Injury Research and Regeneration, J. Neurotrauma 33 (15) (2016) 1405–1415.
[30] N.J. Schaub, T. Britton, R. Rajachar, R.J. Gilbert, Engineered nanotopography on electrospun PLLA microfibers modifies RAW 264.7 cell response, ACS Appl. Mater Interf. 5 (20) (2013) 10173–10184.
[31] C.D. Johnson, A.R. D'Amato, D.L. Puhl, D.M. Wich, A. Vesperman, R.J. Gilbert, Electrospun fiber surface nanotopography influences astrocyte-mediated neurite outgrowth, Biomed. Mater. 13 (5) (2018) 054101.
[32] A.R. D'Amato, D.L. Puhl, A.M. Ziemba, C.D.L. Johnson, J. Doedee, J. Bao, R.J. Gilbert, Exploring the effects of electrospun fiber surface nanotopography on neurite outgrowth and branching in neuron cultures, PLoS ONE 14 (2) (2019) e0211731.
[33] J.M. Corey, D.Y. Lin, K.B. Mycek, Q. Chen, S. Samuel, E.L. Feldman, D.C. Martin, Aligned electrospun nanofibers specify the direction of dorsal root ganglia neurite growth, J. Biomed. Mater. Res., Part A 83A (3) (2007) 636–645.
[34] L. Yao, N. O'Brien, A. Windebank, A. Pandit, Orienting neurite growth in electrospun fibrous neural conduits, J. Biomed. Mater Res. B Appl. Biomater 90 (2) (2009) 483–491.
[35] N. Rangappa, A. Romero, K.D. Nelson, R.C. Eberhart, G.M. Smith, Laminin–coated poly(L-lactide) filaments induce robust neurite growth while providing directional orientation, J. Biomed. Mater. Res. 51 (4) (2000) 625–634.
[36] Y. Ren, D.M. Suter, Increase in Growth Cone Size Correlates with Decrease in Neurite Growth Rate, Neural Plast. 2016 (2016) 13.
[37] C.E. Schmidt, J.B. Leach, Neural tissue engineering: strategies for repair and regeneration, Annu. Rev. Biomed. Eng. 5 (2003) 293–347.
[38] K.M. Rich, T.D. Alexander, J.C. Pryor, J.P. Hollowell, Nerve growth factor enhances regeneration through silicone chambers, Exp. Neurol. 105 (2) (1989) 162–170.
[39] L.R. Williams, Exogenous fibrin matrix precursors stimulate the temporal progress of nerve regeneration within a silicone chamber, Neurochem. Res. 12 (10) (1987) 851–860.
[40] R.F. Valentini, P. Aebischer, S.R. Winn, P.M. Galletti, Collagen- and laminin–containing gels impede peripheral nerve regeneration through semipermeable nerve guidance channels, Exp. Neurol. 98 (2) (1987) 350–356.
[41] J.S.H. Taylor, E.T.W. Bampton, Factors secreted by Schwann cells stimulate the regeneration of neonatal retinal ganglion cells, J. Anat. 204 (1) (2004) 25–31.
[42] X. Wen, P.A. Tresco, Effect of filament diameter and extracellular matrix molecule precoating on neurite outgrowth and Schwann cell behavior on multifilament entubulation bridging device in vitro, J. Biomed. Mater Res. A 76 (3) (2006) 626–637.
[43] J. Xie, M.R. MacEwan, X. Li, S.E. Sakiyama-Elbert, Y. Xia, Neurite Outgrowth on Nanofiber Scaffolds with Different Orders, Structures, and Surface Properties, ACS Nano 3 (5) (2009) 1151–1159.
[44] S.S. Yang, J. Cha, S.-.W. Cho, P. Kim, Time-Dependent Retention of Nanotopographical Cues in Differentiated Neural Stem Cells, ACS Biomater Sci. Eng. 5 (8) (2019) 3802–3807.
[45] C. Yang, M.W. Tibbitt, L. Basta, K.S. Anseth, Mechanical memory and dosing influence stem cell fate, Nat Mater 13 (6) (2014) 645–652.
[46] I. Tonazzini, C. Masciullo, E. Savi, A. Sonato, F. Romanato, M. Cecchini, Neuronal contact guidance and YAP signaling on ultra-small nanogratings, Sci. Rep. 10 (1) (2020) 3742.
[47] A. Elosegui-Artola, I. Andreu, A.E.M. Beedle, A. Lezamiz, M. Uroz, A.J. Kosmalska, R. Oria, J.Z. Kechagia, P. Rico-Lastres, A.L. Le Roux, C.M. Shanahan, X. Trepat, D. Navajas, S. Garcia-Manyes, P. Roca-Cusachs, Force Triggers YAP Nuclear Entry by Regulating Transport across Nuclear Pores, Cell 171 (6) (2017) 1397–1410.
[48] A.K. Yip, A.T. Nguyen, M. Rizwan, S.T. Wong, K.-.H. Chiam, E.K.F. Yim, Anisotropic traction stresses and focal adhesion polarization mediates topography-induced cell elongation, Biomaterials 181 (2018) 103–112.
[49] A. Ray, O. Lee, Z. Win, R.M. Edwards, P.W. Alford, D.-.H. Kim, P.P. Provenzano, Anisotropic forces from spatially constrained focal adhesions mediate contact guidance directed cell migration, Nat Commun. 8 (1) (2017) 14923.
[50] K.E. Kubow, S.K. Conrad, A.R. Horwitz, Matrix microarchitecture and myosin II determine adhesion in 3D matrices, Current Biol. CB 23 (17) (2013) 1607–1619.
[51] A. Rajnicek, S. Britland, C. McCaig, Contact guidance of CNS neurites on grooved quartz: influence of groove dimensions, neuronal age and cell type, J. Cell Sci. 110 (Pt 23) (1997) 2905–2913.
[52] P. Clark, P. Connolly, A.S. Curtis, J.A. Dow, C.D. Wilkinson, Topographical control of cell behaviour. I. Simple step cues, Development 99 (3) (1987) 439–448.
[53] O. Shefi, I. Golding, R. Segev, E. Ben-Jacob, A. Ayali, Morphological characterization of in vitro neuronal networks, Phys. Rev. E Stat. Nonlin Soft Matter Phys. 66 (2 Pt 1) (2002) 021905.
[54] J. Cove, P. Blinder, E. Abi-Jaoude, M. Lafreniere-Roula, L. Devroye, D. Baranes, Growth of neurites toward neurite- neurite contact sites increases synaptic clustering and secretion and is regulated by synaptic activity, Cereb Cortex 16 (1) (2006) 83–92.
[55] V. Sytnyk, I. Leshchyns'ka, M. Delling, G. Dityateva, A. Dityatev, M. Schachner, Neural cell adhesion molecule promotes accumulation of TGN organelles at sites of neuron-to-neuron contacts, J. Cell Biol. 159 (4) (2002) 649–661.
[56] O. Shefi, S. Golebowicz, E. 9, A. Ayali, A two-phase growth strategy in cultured neuronal networks as reflected by the distribution of neurite branching angles, J. Neurobiol. 62(3) (2005) 361–8.
[57] O. Shefi, E. Ben-Jacob, A. Ayali, Growth morphology of two-dimensional insect neural networks, Neurocomputing 44-46 (2002) 635–643.
[58] H. Chen, X. Huang, M. Zhang, F. Damanik, M.B. Baker, A. Leferink, H. Yuan, R. Truckenmüller, C. van Blitterswijk, L. Moroni, Tailoring surface nanoroughness of electrospun scaffolds for skeletal tissue engineering, Acta Biomater 59 (2017) 82–93.